



**HAL**  
open science

# Global Analysis of Surface Ocean CO<sub>2</sub> Fugacity and Air-Sea Fluxes With Low Latency

Thi-tuyet-trang Chau, Frédéric Chevallier, Marion Gehlen

► **To cite this version:**

Thi-tuyet-trang Chau, Frédéric Chevallier, Marion Gehlen. Global Analysis of Surface Ocean CO<sub>2</sub> Fugacity and Air-Sea Fluxes With Low Latency. *Geophysical Research Letters*, 2024, 51 (8), 10.1029/2023gl106670 . hal-04573078

**HAL Id: hal-04573078**

**<https://hal.science/hal-04573078>**

Submitted on 13 May 2024

**HAL** is a multi-disciplinary open access archive for the deposit and dissemination of scientific research documents, whether they are published or not. The documents may come from teaching and research institutions in France or abroad, or from public or private research centers.

L'archive ouverte pluridisciplinaire **HAL**, est destinée au dépôt et à la diffusion de documents scientifiques de niveau recherche, publiés ou non, émanant des établissements d'enseignement et de recherche français ou étrangers, des laboratoires publics ou privés.

# Geophysical Research Letters<sup>®</sup>

## RESEARCH LETTER

10.1029/2023GL106670

## Global Analysis of Surface Ocean CO<sub>2</sub> Fugacity and Air-Sea Fluxes With Low Latency



### Key Points:

- We demonstrate the capacity of statistical models to generate global maps of  $f\text{CO}_2$  and air-sea flux with a latency reduced to one month
- A decrease in the CO<sub>2</sub> source for January to August 2023 diagnosed in the tropical Pacific coheres with the retreat of the La Niña event
- An unusual northeastern Atlantic sink reduction diagnosed for June 2023 is linked to record heat and exceptionally low winds

### Supporting Information:

Supporting Information may be found in the online version of this article.

### Correspondence to:

T.-T.-T. Chau,  
thi.tuyet.trang.chau@gmail.com

### Citation:

Chau, T.-T.-T., Chevallier, F., & Gehlen, M. (2024). Global analysis of surface ocean CO<sub>2</sub> fugacity and air-sea fluxes with low latency. *Geophysical Research Letters*, 51, e2023GL106670. <https://doi.org/10.1029/2023GL106670>

Received 5 OCT 2023

Accepted 15 FEB 2024

### Author Contributions:

**Conceptualization:** Thi-Tuyet-Trang Chau, Frédéric Chevallier, Marion Gehlen

**Formal analysis:** Thi-Tuyet-Trang Chau

**Investigation:** Thi-Tuyet-Trang Chau, Frédéric Chevallier, Marion Gehlen

**Methodology:** Thi-Tuyet-Trang Chau, Frédéric Chevallier, Marion Gehlen

**Project administration:** Frédéric Chevallier, Marion Gehlen

**Resources:** Thi-Tuyet-Trang Chau, Frédéric Chevallier, Marion Gehlen

**Software:** Thi-Tuyet-Trang Chau

**Supervision:** Frédéric Chevallier, Marion Gehlen

**Validation:** Thi-Tuyet-Trang Chau, Frédéric Chevallier, Marion Gehlen

**Visualization:** Thi-Tuyet-Trang Chau

© 2024. The Authors.

This is an open access article under the terms of the [Creative Commons Attribution License](#), which permits use, distribution and reproduction in any medium, provided the original work is properly cited.

Thi-Tuyet-Trang Chau<sup>1</sup> , Frédéric Chevallier<sup>1</sup> , and Marion Gehlen<sup>1</sup> 

<sup>1</sup>Laboratoire des Sciences du Climat et de l'Environnement, LSCE/IPSL, CEA-CNRS-UVSQ, Université Paris-Saclay, Gif-sur-Yvette, France

**Abstract** The Surface Ocean CO<sub>2</sub> Atlas (SOCAT) of CO<sub>2</sub> fugacity ( $f\text{CO}_2$ ) observations is a key resource supporting annual assessments of CO<sub>2</sub> uptake by the ocean and its side effects on the marine ecosystem. SOCAT data are usually released with a lag of up to 1.5 years which hampers timely quantification of recent variations of carbon fluxes between the Earth System components, not only with the ocean. This study uses a statistical ensemble approach to analyze  $f\text{CO}_2$  with a latency of one month only based on the previous SOCAT release and a series of predictors. Results indicate a modest degradation in a retrospective prediction test for 2021–2022. The generated  $f\text{CO}_2$  and fluxes for January–August 2023 show a progressive reduction in the Equatorial Pacific source following the La Niña retreat. A breaking-record decrease in the northeastern Atlantic CO<sub>2</sub> sink has been diagnosed on account of the marine heatwave event in June 2023.

**Plain Language Summary** There is a growing need to monitor carbon emissions and removals over the globe in near real time in order to correctly interpret changes in CO<sub>2</sub> concentrations as they unfold. For the oceans, the best information comes from measurements of the surface ocean CO<sub>2</sub> fugacity ( $f\text{CO}_2$ ) by the international marine carbon research community. So far, this data is mostly available 6 to 18 months behind real time after collection, qualification, harmonization, and processing. Here, we show that a set of biological, chemical, and physical predictors available in near real time, allows the information contained in the “old”  $f\text{CO}_2$  measurements to be transferred over time. Based on a statistical technique, we combine all these data sources to estimate global monthly maps of  $f\text{CO}_2$  and of CO<sub>2</sub> fluxes at the air-sea interface within one month behind real time and with good accuracy.

## 1. Introduction

The ocean is a sink taking up about 26% of atmospheric carbon dioxide (CO<sub>2</sub>) and 90% of the heat induced largely by anthropogenic greenhouse gas emissions (Canadell et al., 2021; Friedlingstein et al., 2022). The global ocean carbon sink is proportional to CO<sub>2</sub> human emissions only at the decadal scale. On shorter time scales, it varies with the climate (mostly temperature and winds), with a dependency that also varies from basin to basin given their respective geographical, dynamic, and biological specificities (Gruber et al., 2023; Landschützer et al., 2016; Rödenbeck et al., 2015).

Measurements of surface ocean CO<sub>2</sub> fugacity ( $f\text{CO}_2$ ) from ships, drifters, moorings, and autonomous surface platforms are the main reference to document the actual variation of air-sea fluxes ( $f_g\text{CO}_2$ ) in space and time (Friedlingstein et al., 2022) because the two are linearly related. Long-term efforts in maintaining and expanding international observing networks together with a coordinated data aggregation of the Surface Ocean CO<sub>2</sub> Atlas database - SOCAT (Bakker et al., 2016, 2023) have provided millions of individual  $f\text{CO}_2$  observations since the 1950s and associated gridded products. However,  $f\text{CO}_2$  data are poorly sampled leaving out most areas for some or all of the year. Statistical data-based and machine-learning-based reconstructions of  $f\text{CO}_2$  (Chau et al., 2022b; Gregor & Gruber, 2021; Landschützer et al., 2016; Rödenbeck et al., 2013) have emerged to gap-fill the SOCAT database using auxiliary data, resulting in reconstructions of  $f\text{CO}_2$  global monthly maps. They are still the topic of active research to improve the reconstruction quality, but these maps lag behind real time by 0.5–1.5 years: the update of the SOCAT archive follows an annual pace with a public release usually in June after measurement collection, quality control, and processing. This lag is problematic for the documentation of the carbon cycle as it evolves, while the main variables of the carbon cycle like atmospheric concentrations, emissions, and absorptions from the terrestrial biosphere or fossil fuel emissions, are progressively integrated within operational programmes with much faster data releases. A prominent example of operational programmes in need of a reduced time lag is

**Writing – original draft:** Thi-Tuyet-Trang Chau, Frédéric Chevallier, Marion Gehlen

**Writing – review & editing:** Thi-Tuyet-Trang Chau, Frédéric Chevallier, Marion Gehlen

the operational observation-based anthropogenic CO<sub>2</sub> emissions monitoring and verification support capacity (CO<sub>2</sub>MVS) that the European Commission is building under its Copernicus Earth Observation program (e.g., Janssens-Maenhout et al. (2020)). As its observational component relies heavily on satellite observations of CO<sub>2</sub> in the atmosphere, which is affected by the ocean as well as terrestrial emissions and removals, better estimates of *f*CO<sub>2</sub> would result in efficient estimates of air-sea fluxes and thence benefit air-land flux accuracy, in addition to being directly interesting to users. The CO<sub>2</sub>MVS fits within the Global Greenhouse Gas Watch, an even larger greenhouse gas monitoring infrastructure that the World Meteorological Organization (WMO) is setting up (<https://wmo.int/news/media-centre/world-meteorological-congress-approves-global-greenhouse-gas-watch>, last access: 12/12/2023).

Here, we demonstrate the capability to retrieve global monthly maps of *f*CO<sub>2</sub> from SOCAT data and then to generate the corresponding fields of air-sea fluxes with a lag reduced to one month. To do that, we extend the work of Chau et al. (2022b) who have been gap-filling SOCAT gridded data within the framework of the Copernicus Marine Environment Monitoring Service (CMEMS) based on an ensemble of feed-forward neural network models (also referred to as CMEMS-LSCE-FFNN) and a set of biological, chemical, and physical predictors (see Section 2). While Chau et al. (2022b) made the dates of the predictors and the date of the gridded SOCAT data coincide, we turn to a prediction mode in which the relationship found between the predictors and the SOCAT data more than 6 months before is kept. Section 2 below describes the method. We test the approach in the years 2021–2022 by examining the retrospective prediction skill based on the available SOCAT data. Then we expand model prediction of *f*CO<sub>2</sub> and generate *f*gCO<sub>2</sub> up to present with a latency of 1 month: data access via the LSCE data center, [https://dods.lsce.ipsl.fr/invsat/FFNN\\_low-latency/](https://dods.lsce.ipsl.fr/invsat/FFNN_low-latency/). The results include the finding of anomalous variations in CO<sub>2</sub> uptake and release by the Equatorial Pacific and the North Atlantic Ocean predicted in January to August 2023, as described in Section 3. Section 4 draws the main conclusions of the study.

## 2. Materials and Methods

CMEMS-LSCE-FFNN (Chau et al., 2022b) is built on machine-learning techniques. It consists of an ensemble of feed-forward neural network (FFNN) models. This ensemble approach was developed at LSCE in order to reconstruct surface ocean carbonate system variables and to support the operational distribution of such data sets by CMEMS since 2019 (Product identity: MULTIOBS\_GLO\_BIO\_CARBON\_SURFACE\_REP\_015\_008, Chau et al., 2022a). The original CMEMS-LSCE-FFNN fields cover the global ocean at a resolution of 1° × 1° and for the period since the year 1985 at monthly resolution.

Under the hood, these FFNN models represent nonlinear mappings of *f*CO<sub>2</sub> against a set of predictors. Monthly gridded observation-based products of *f*CO<sub>2</sub> from SOCAT (Bakker et al., 2016) are used as the target data in model fitting. *f*CO<sub>2</sub> predictors are environmental variables: sea surface temperature (SST), sea surface salinity (SSS), sea surface height (SSH), chlorophyll-*a* (Chl-*a*), mix-layer-depth (MLD), CO<sub>2</sub> surface mole fractions (*x*CO<sub>2</sub>), climatological *f*CO<sub>2</sub> (*f*CO<sub>2</sub><sup>clim</sup>), and geographical coordinates (latitude and longitude). Product resources of input data sets are detailed in Table S1 in Supporting Information S1. CMEMS-LSCE-FFNN comprises monthly adaptive FFNN models for which the *f*CO<sub>2</sub> and predictor data sets available within a time span of 3 months for all the years since 1985 (the reconstruction month excepted) are used in the fitting phase. SOCAT *f*CO<sub>2</sub> in the reconstruction month is only used in model evaluation. The ensemble of multi-FFNN models was designed by randomly splitting two thirds of the 3-month sliding data sets for training and the rest for model test (Chau et al., 2022b). From the ensemble reconstructions, the model best estimate (ensemble mean) and 1σ—model uncertainty (ensemble standard deviation) of *f*CO<sub>2</sub> are derived at the desired resolution.

Here we revisit the two versions of CMEMS-LSCE-FFNN referred to as FFNNv2021 and FFNNv2022. These two models respectively used SOCATv2021 and SOCATv2022 data sets (Bakker et al., 2021, 2022) as the target input data of *f*CO<sub>2</sub>. Note that SOCAT has been annually published in mid-June. Due to the delay mode for data collection, reprocessing, and quality control, SOCAT provides gridded data up to the year before the publication date (see Bakker et al. (2016, 2023) for instance). For the period 1985–2021, SOCATv2022 offers an amount of roughly 311,700 monthly 1-degree gridded data, 5,000 more than SOCATv2021 (Table S3a in Supporting Information S1). The data increase in SOCATv2022 is mostly distributed within the last three years due to the late availability of some data sources (Figure 1). However, SOCATv2021 has more data before 2018, up to at least

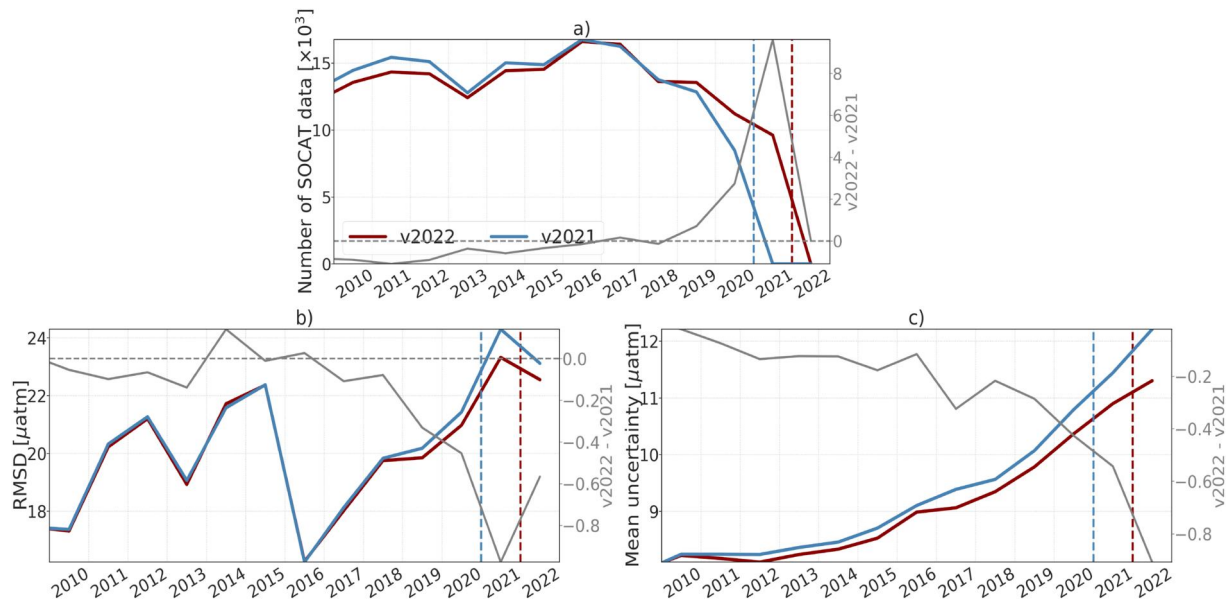


**Figure 1.** (a) Number of data per year in SOCATv2021 and SOCATv2022, (b) RMSD of FFNNv2021 and FFNNv2022 against SOCATv2023  $f\text{CO}_2$ , (c) yearly global mean uncertainty ( $1\sigma$ ). Differences between the two versions are shown with a gray solid curve with values on the right y-axis whereas the gray solid curve below 0 (gray dashed horizontal line). The blue and red vertical lines mark the start of the prediction mode for FFNNv2021 and FFNNv2022, respectively.

1000 more in some years (e.g., 2011 and 2012) due to an erroneous flagging of some data (Bakker et al., 2021). Despite this feature, the two corresponding FFNN reconstructions do not exhibit large systematic offsets in their  $f\text{CO}_2$  estimates (Chau et al., 2022a).

For all experiments in this study, the ensemble size (i.e., number of FFNN model runs) is set to 50. FFNN with 50 ensemble members has less computational complexity than with the usual size of 100 but it shows similar reconstruction skill (Chau et al., 2022b). The same input data of predictors is fed to the two FFNN model runs (Table S1 in Supporting Information S1). The FFNNv2021 (respectively FFNNv2022) model relies on SOCATv2021 (respectively SOCATv2022) and predictor data sets in 1985–2020 (respectively 1985–2021). This allows deriving the ensemble global reconstructions of  $f\text{CO}_2$  over the 36-year and 37-year periods, accordingly. The ensemble of FFNN models is then applied to predict  $f\text{CO}_2$  given the set of predictors in the years 2021–2022 for version 2021 and in the year 2022 for the latter. The quality assessments are made for (a) the two global reconstructions in the period 1985–2020, (b) FFNNv2021 one-year prediction against FFNNv2022 one-year reconstruction in 2021, and (c) FFNNv2021 two-year prediction against FFNNv2022 one-year prediction in 2022. Model performances will be qualified with the latest SOCAT data, that is, SOCATv2023 (Bakker et al., 2023). The number of evaluation data for prediction in the years 2021 and 2022 over the global ocean is 10,908 and 8,602, respectively (Table S3a in Supporting Information S1), which is statistically sufficient for significant validation.

Model skills are examined from global to sub-basin scale. Here we consider the sub-basins defined by the Gregor (2022). Due to a lack of evaluation data in several RECCAP2 biomes, we aggregate some of them, yielding 14 provinces in total (see Table S2 and Figure S1 in Supporting Information S1): Arctic (1. ARC), North Atlantic seasonally stratified (2. NA-SS), North Atlantic permanently stratified (3. NA-PS), Atlantic equatorial (4. AEQU), South Atlantic (5. SA), North Pacific seasonally stratified (6. NP-SS), North Pacific permanently stratified (7. NP-PS), Pacific western equatorial (8. PEQU-W), Pacific eastern equatorial (9. PEQU-E), South Pacific (10. SP), Northern Indian Ocean (11. NIO), Southern Indian Ocean (12. SIO), Southern Ocean seasonally stratified (13. SO-SS), Southern Ocean ice (14. SO-ICE). These ocean provinces, therefore, differ from the original biomes proposed by Fay and McKinley (2014). Apart from the NIO, the number of data for prediction evaluation ranges from 133 (12. SIO) to 2350 (2. NA-SS) in the year 2021 and from 73 to 2265 in the year 2022.

For the actual prediction in 2022 and 2023, the latest model (FFNNv2022) has been run given monthly data of predictors (Table S1 in Supporting Information S1) in the year 2022 to present. We choose to release the maps of  $f\text{CO}_2$  and  $f_g\text{CO}_2$  for the previous month on the 15th of each month.

### 3. Evaluation and Discussions

#### 3.1. Reconstruction and Prediction of $\text{CO}_2$ Fugacity in 1985–2022

##### 3.1.1. Global Qualification

FFNNv2021 and FFNNv2022 share consistent global RMSD and determination coefficient  $r^2$  (Figure 1 and Table S3 in Supporting Information S1). Between 1985 and 2020, the two reconstructions inherit the same RMSD of 19.1  $\mu\text{atm}$  and  $r^2$  of 0.78 (Table S3b in Supporting Information S1). Improvement in the global reconstruction skill of FFNNv2022 in recent years (Figure 1b) is moderate despite 5,000 additional  $f\text{CO}_2$  data in the model training (Figure 1a). In detail, these 1.7% additional data in SOCATv2022 (311,694 in total) in 1985–2021 correspond to 9,615 data added in 2021 and 4,278 data removed from SOCATv2021 in 1985–2020 (see the spatial distribution of removal data in Figure S2c in Supporting Information S1).

The RMSD variability before 2018 (Figure 1b) is likely linked to changes in the data sampling in regions with high spatiotemporal variability of  $f\text{CO}_2$  (see Gregor et al. (2019); Chau et al. (2022b) for further analysis). However, the difference between the RMSD of the two reconstructions is negligible then, as it fluctuates within  $[-0.1, 0.1]$   $\mu\text{atm}$ . During the last four years, a monotonous increase in RMSD (Figure 1b) coexists with a decrease in the number of SOCAT data (Figure 1a), and the FFNNv2021 reconstruction slightly, but increasingly, underperforms compared to FFNNv2022. In 2021 and 2022, the FFNNv2021 prediction RMSD is 24.3 and 23.1  $\mu\text{atm}$ , respectively, roughly 0.5–1  $\mu\text{atm}$  higher than that of the FFNNv2022 reconstruction and prediction (Table S3 in Supporting Information S1). Likewise, the variation of SOCAT  $f\text{CO}_2$  is reproduced with high  $r^2$  values (0.74 and 0.75), close to the one-year reconstruction and prediction of FFNNv2022 (0.76) for the years 2021–2022.

The yearly-mean uncertainty over the global ocean (Figure 1c) is computed by weighting the model estimated uncertainty (ensemble spread) per grid cell ( $\sigma$ ) with the geographical area. The two reconstructions before the year 2015 are rather stable with an uncertainty about 8.5  $\mu\text{atm}$ . The increase in FFNNv2021 [v2022] model uncertainty from 8.7  $\mu\text{atm}$  [8.5  $\mu\text{atm}$ ] to 10.8  $\mu\text{atm}$  [10.4  $\mu\text{atm}$ ] between 2015 and 2020 follows a decrease in observation-based data from 14,877 [14,533] to 8,482 [11,217] (Figure 1a). In the year 2021, the FFNNv2021 uncertainty of predicted  $f\text{CO}_2$  (11.4  $\mu\text{atm}$ ) is slightly higher than that of the FFNNv2022 reconstruction but the offset between the two values is as small as 0.5  $\mu\text{atm}$  (Figure 1c). The prediction uncertainty in 2022 increases by 0.4–0.8  $\mu\text{atm}$  for the two models (FFNNv2021: 12.2  $\mu\text{atm}$ , FFNNv2022: 11.3  $\mu\text{atm}$ ).

##### 3.1.2. Regional Assessment

Model reconstruction and prediction skills are assessed over 14 ocean provinces (Figures S1 and S2 in Supporting Information S1) in the years 1985–2020 and 2021–2022 (1985–2021 and 2022) for FFNNv2021 (FFNNv2022). Results of the regional evaluation are summarized in Figure 2 and Table S4 in Supporting Information S1. The two FFNN models perform with a similar skill in reconstruction mode (1985–2020) over all ocean provinces. Evidently, their reconstructions share consistent patterns in regional-mean  $f\text{CO}_2$  (Figure 2b) and in the spatial and temporal variations (Figures S4a–S4c and S7 in Supporting Information S1) with systematic biases below 1  $\mu\text{atm}$  for most of the basins (Table S4 in Supporting Information S1). Differences in uncertainty estimates and RMSD do not exceed 0.5  $\mu\text{atm}$  while those in  $r^2$  are nearly the same (Figures 2c–2e and Table S4 in Supporting Information S1).

In the years 2021–2022, RMSD ( $r^2$ ) of the FFNN prediction does not change from the full-period reconstruction by more than about 5  $\mu\text{atm}$  (0.1) over many sub-basins (e.g., 2.NA-SS, 7.NP-PS, 8.PEQU-W, 10.SP, 12.SIO, and 13.SO-SS). As expected, FFNNv2022 (one-year prediction) performs slightly better than FFNNv2021 (two-year prediction) in the 2022 prediction for many regions (Figures 2d and 2e and Table S4 in Supporting Information S1). However, the differences in regional skill scores of the two models are substantially small, that is, below 3  $\mu\text{atm}$  for RMSD and 0.05 for  $r^2$ . These results suggest a high confidence level in FFNN prediction for a few years ahead. The analysis of the spatial distribution and of the time series (Figure 2, Figures S4, and S7 in Supporting Information S1) also reveals consistent features (horizontal gradients of  $f\text{CO}_2$  and seasonality to long-

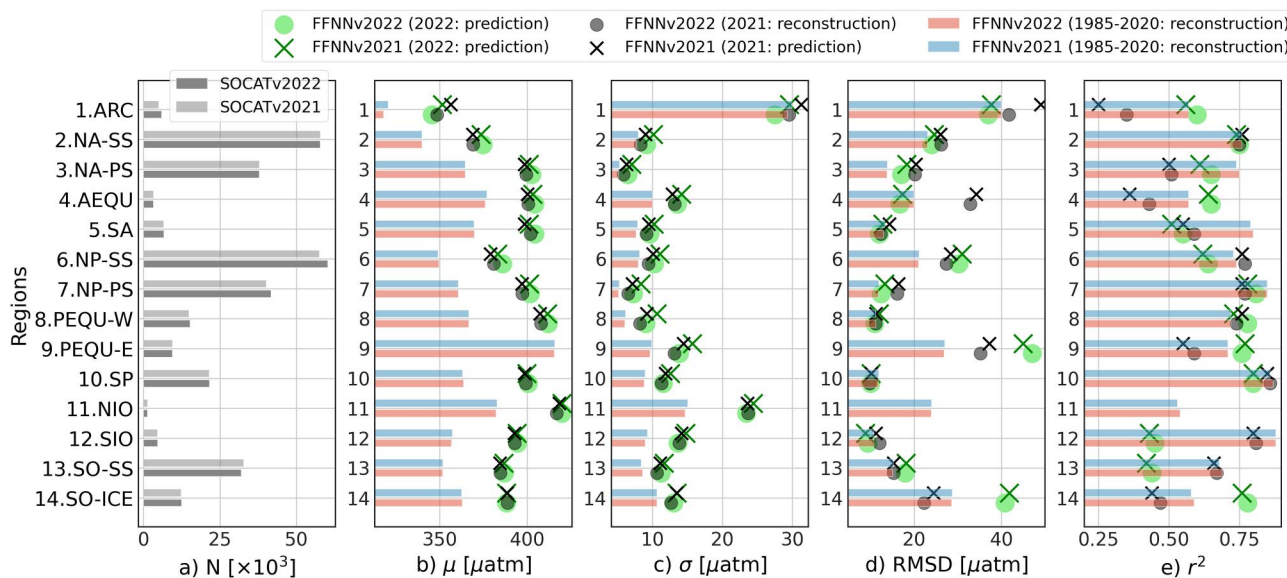


**Figure 2.** Regional comparisons of the two FFNN reconstructions in 1985–2020 (bars) and of the FFNNv2021 prediction versus the FFNNv2022 reconstruction [prediction] in 2021 [2022] (objects) in terms of (a) N- number of SOCAT monthly gridded data used in model fitting, (b)  $\mu$ -mean  $f\text{CO}_2$ , (c)  $\sigma$ -mean uncertainty, (d) RMSD model-data deviation, and (e)  $r^2$  model-data correlation.

term variations) from the reconstruction years to the prediction years.  $f\text{CO}_2$  increases over time (see f.i., 7.NP-PS, 8.PEQU-W, 12.SIO) following the trend in atmospheric  $\text{CO}_2$  concentration. Among the  $f\text{CO}_2$  predictors,  $x\text{CO}_2$  stands out with its large increasing trend that brings some  $x\text{CO}_2$  data used in the prediction above the range of those used in the training. The growth of atmospheric  $\text{CO}_2$  is the primary factor driving the increase in sea surface  $f\text{CO}_2$  (Bates et al., 2014; Friedlingstein et al., 2022; Gruber et al., 2019; Landschützer et al., 2019). The prediction skill, however, does not degrade compared to the reconstruction as the annual increment of  $f\text{CO}_2$  is typically smaller than its intra-annual variability (Figure S6 in Supporting Information S1). The latter is dominantly driven by temperature-dependent  $\text{CO}_2$  solubility and biological processes (Gallego et al., 2018; Rustogi et al., 2023; Takahashi et al., 2002). The range of the pre-2021 [pre-2022] training data sets of physical and biological predictors (e.g., SST, Chl- $a$ ) remains similar to that including input data in the next year. Seasonality and multi-month variations of  $f\text{CO}_2$  in the years 2021–2022 can be, therefore, propagated with these covariates overall. The majority of SOCAT  $f\text{CO}_2$  data for 2021 [2022] stays within the full range of training data which also supports FFNNs to achieve a skillful prediction (Figure S3 in Supporting Information S1). Further analysis of FFNN prediction skills over ocean basins is presented in Supporting Information S1.

### 3.2. Prediction of Air-Sea $\text{CO}_2$ Fluxes in 2022–2023

The previous results emphasize the skill and reliability of FFNN models in both reconstruction and prediction of  $\text{CO}_2$  fugacity ( $f\text{CO}_2$ ). In this section, we will use the FFNNv2022 predicted  $f\text{CO}_2$  field to generate corresponding air-sea fluxes ( $fg\text{CO}_2$ ) and analyze preliminary results for 20 months, from January 2022 to August 2023.  $fg\text{CO}_2$  is given in  $\text{molC.m}^{-2}.\text{yr}^{-1}$  for a flux density and in  $\text{PgC.yr}^{-1}$  for integration over ocean basins (see Section S1.2 in Supporting Information S1 for details of flux calculation and analysis). FFNNv2022 predicts a reduction in the global ocean uptake of  $\text{CO}_2$  for 2022 ( $2.25 \pm 0.5 \text{ PgC.yr}^{-1}$ ) compared to the previous year ( $2.36 \pm 0.43 \text{ PgC.yr}^{-1}$ ). When adjusting the estimated global net fluxes with the riverine outgassing of  $\text{CO}_2$  of  $0.65 \text{ PgC.yr}^{-1}$  (Regnier et al., 2022) and the total ocean surface area (FFNNv2022 data covers 95% of the global ocean), one obtains the estimates of anthropogenic ocean carbon uptake consistent with the 2022 projection proposed by Friedlingstein et al. (2022): the anthropogenic ocean sink in 2021 was  $2.9 \pm 0.4 \text{ PgC.yr}^{-1}$  remains unchanged for the year 2022. This evidence supports their hypothesis that the persistence of cooling climate patterns (La Niña conditions) weakened  $\text{CO}_2$  ocean uptake in 2021–2022 (high peaks appeared mid-2022, Figure S9 in Supporting Information S1). FFNNv2022 predicts a global net flux of  $2.45 \pm 0.56 \text{ PgC.yr}^{-1}$  for January to August 2023, the enhancement of global ocean uptake compared to that in 2022 ( $2.17 \pm 0.50 \text{ PgC.yr}^{-1}$ ) is synchronous with the retreat of La Niña.

The model prediction retains the seasonal to interannual variations of  $f\text{CO}_2$  and  $fg\text{CO}_2$  in the pre-2022 reconstruction over many ocean basins (Figures S6 and S8 in Supporting Information S1). One of the remarkable changes is observed at the equatorial Atlantic (4.AEQU), where the regional mean  $f\text{CO}_2$  increases by  $4.2 \mu\text{atm}$  from the year 2021–2022 (Figure S6 in Supporting Information S1). However, such a high increment in the AEQU  $f\text{CO}_2$  is negligible in terms of its contribution to the global net ocean sink variations between the two years (Figure S8 and Table S5 in Supporting Information S1). In Rödenbeck et al. (2015, Figures A2 and A4), it is also illustrated that  $p\text{CO}_2^{\text{sea}}$  ranges from 350 to 400  $\mu\text{atm}$  over an 18-year period while the AEQU net flux has performed with nearly constant magnitude. Its low interannual variability is in contrast with the eastern equatorial Pacific (9.PEQU-E) showing the strong impact on temporal variations of the global net sink (Figure S8 in Supporting Information S1). The signature of  $f\text{CO}_2$  dampening ( $-9.4 \mu\text{atm}$ ) over PEQU-E in Jan to August of 2022–2023 is opposed to its increasing ( $1.8 \mu\text{atm}$ ) with respect to 2021–2022 (Figure S6 in Supporting Information S1). As illustrated in Figures S8 and S9 in Supporting Information S1, FFNNv2022 prediction marks an anomalous decline of  $\text{CO}_2$  source in the first eight months of 2023 ( $-0.30 \pm 0.04 \text{ PgC.yr}^{-1}$ ) compared to that of 2022 ( $-0.37 \pm 0.04 \text{ PgC.yr}^{-1}$ ). This reduced source of  $0.07 \text{ PgC.yr}^{-1}$  in PEQU-E contributes to 25% of the increase in the global ocean sink mentioned above. The reduction in the PEQU-E  $\text{CO}_2$  source marks the transition from La Niña to El Niño announced by for example, WMO (<https://wmo.int/news/media-centre/world-meteorological-organization-declares-onset-of-el-nino-conditions>, last access: 22/02/2024).

While the onset of El Niño over the tropical Pacific (Figure S9a in Supporting Information S1) had been driving the reduction of ocean  $\text{CO}_2$  emission La Niña anomalies (Figure S8 in Supporting Information S1), an exceptional warming event occurred and spread over the north Atlantic since May–June 2023 (Copernicus Climate Change Service: <https://climate.copernicus.eu/copernicus-record-north-atlantic-warmth-hottest-june-record-globally>, last access: 20/09/2023). It substantially lessened the ocean  $\text{CO}_2$  uptake (Figure 3). Based on the CMEMS SST analyses (Table S1 in Supporting Information S1), June 2023 corresponds to the first marine extreme heatwave in the northeastern Atlantic ( $40^\circ\text{W}$ – $12^\circ\text{E}$ ,  $5^\circ\text{N}$ – $65^\circ\text{N}$ ) with an average SST anomaly about  $1.1^\circ\text{C}$  (Figures 3a and 3e in Supporting Information S1). As a comparison, the June anomaly had been typically in a range of  $-0.5^\circ\text{C}$  to  $0.5^\circ\text{C}$  for the past three decades. In 2023, SST anomalies even exceeded  $1.5^\circ\text{C}$  over the NA-SS province ( $36^\circ\text{N}$  northward). FFNNv2022 predicts an enhancement in  $f\text{CO}_2$  (Figure 3c) following the anomalous warmth in the northeastern Atlantic which is not seen in June 2022 (Figure 3a). As other environmental factors (e.g., salinity and chlorophyll-*a*) have no remarkable anomalies over this ocean basin (Figure S10 in Supporting Information S1), warming primarily reduces  $\text{CO}_2$  solubility and that leads to substantially high surface partial pressure of  $\text{CO}_2$  (Figure 3c).  $f\text{CO}_2$  anomalies were mostly between 4 and 12  $\mu\text{atm}$  in the subtropics and increased eastward. FFNNv2022 records the largest  $f\text{CO}_2$  anomalies in the southeast of NA-SS toward the European coast with values above 16  $\mu\text{atm}$ . Consequently, the predicted air-sea fluxes in June 2023 (Figure 3d) suggest lower-than-average  $\text{CO}_2$  uptake capability. While  $fg\text{CO}_2$  slightly decreased throughout the NA-PS, an anomalous drawdown is found in the NA-SS exceeding  $-0.6 \text{ molC.m}^{-2}.\text{yr}^{-1}$  (equivalent to roughly a reduction in ocean  $\text{CO}_2$  uptake of  $0.11 \text{ PgC.yr}^{-1}$ ). It is noteworthy that a decline in ocean  $\text{CO}_2$  uptake is strengthened if surface wind speeds (*U*) are lowering and  $f\text{CO}_2$  increases. Accompanied by the largest positive SST anomaly in June 2023, there is an unusual reduction in wind intensity, that is, *U* anomalies potentially below  $-1.2 \text{ m.s}^{-1}$  as illustrated in Figure 3b. Overall, regional seasonal cycles plotted for each year show the 2023 SST mostly greater than past values (Figure 3e). The most striking warmth recorded in June 2023 was at  $1.24^\circ\text{C}$  above that in June 2022. July and August 2023 followed up with SST increasing but the SST values are less different from 2022 then ( $1.06^\circ\text{C}$  and  $0.59^\circ\text{C}$  respectively). Also in June 2023, wind speed dropped out of the lower bound of all seasonal cycles and the difference from the previous year was about  $-1.26 \text{ m.s}^{-1}$  (Figure 3f). The combined anomalies in June 2023 marine extreme heat waves set the northeastern Atlantic ocean sink from an enhanced sink in 2022 ( $0.29 \text{ PgC.yr}^{-1}$ ) back to its magnitude in the 2000s ( $0.18 \text{ PgC.yr}^{-1}$ ) (Figure 3g).

#### 4. Conclusions and Perspectives

This study first examined the skill of CMEMS-LSCE-FFNN, an ensemble approach of feed-forward neural networks (FFNN) developed by Chau et al. (2022b), in a retrospective prediction of  $\text{CO}_2$  fugacity ( $f\text{CO}_2$ ) over the global ocean. The assessment was done for two FFNN models. While the latest version (FFNNv2022) trained on SOCATv2022 data for the period 1985–2021 was used to predict  $f\text{CO}_2$  in 2022, FFNNv2021 trained on SOCATv2021 in 1985–2020 was used to predict  $f\text{CO}_2$  in 2021–2022 allowing the qualification of the two-year

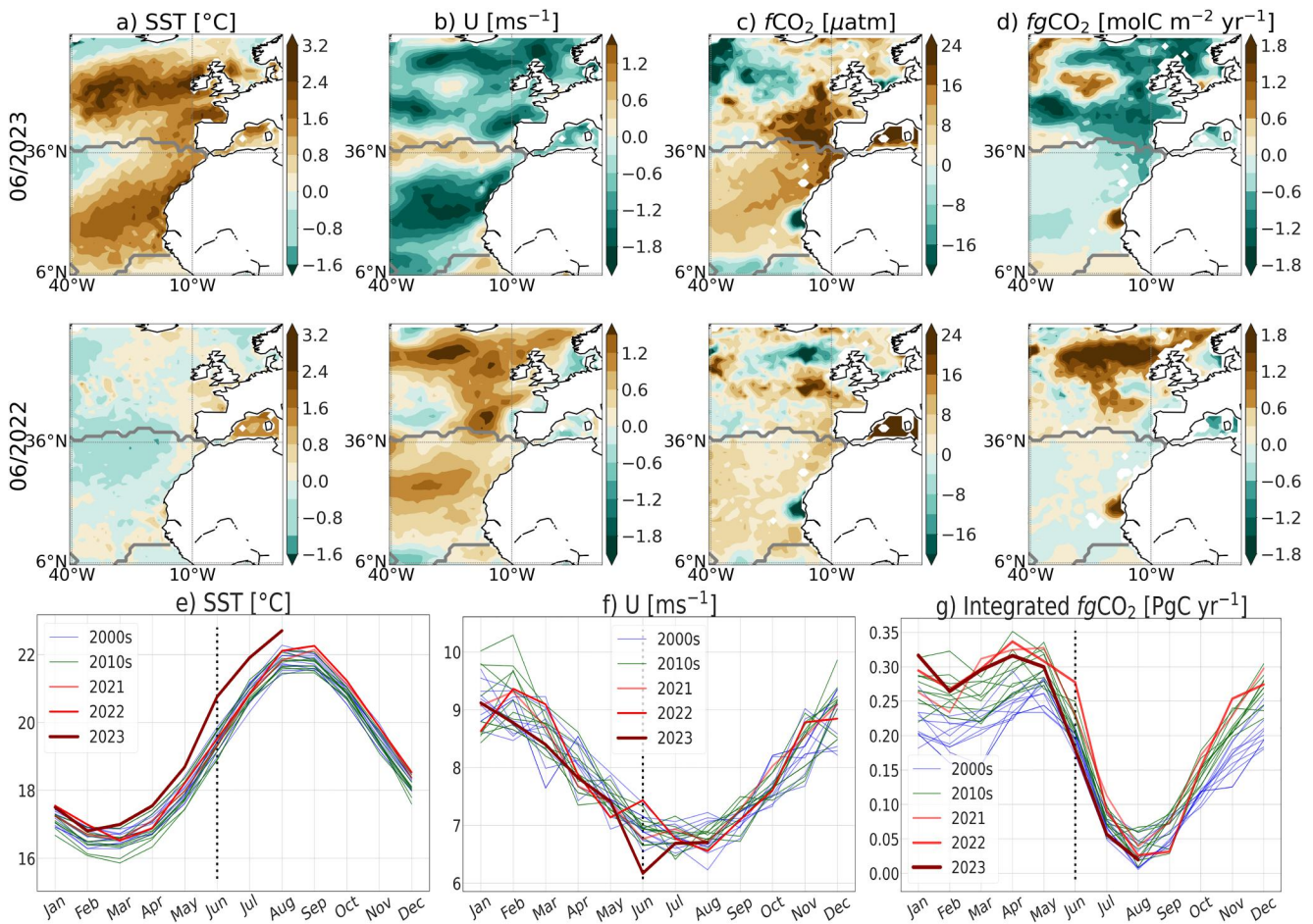


**Figure 3.** Top panels (a–d): anomalies observed in FFNNv2022 prediction of  $f\text{CO}_2$  and  $fg\text{CO}_2$  (c, d) follow an extreme marine heatwave event (a, b) over the northeastern Atlantic in June 2023 relative to June 2022 (top panels). Anomalies of surface temperature (SST), wind speed (U),  $f\text{CO}_2$ , and  $fg\text{CO}_2$  are computed by subtracting long-term trends and seasonal climatologies relative to the years 1985–2022. Gray curve represents a regional division (Figure S1 in Supporting Information S1). Bottom panels (e–g): regional seasonal cycles of SST, U, and integrated air-sea fluxes since 2000s.

model prediction. SOCATv2023 with data available in the prediction years was used for the prediction assessment. Our evaluation confirms a robust performance of the FFNN prediction in comparison to independent observation-based data and to the FFNN reconstruction. The retrospective prediction for the years 2021–2022 retained intra-seasonal to interannual variations of  $f\text{CO}_2$  as those in the reconstruction time series and no large systematic bias has been observed between the two across all ocean provinces. The closeness between the predicted and reconstructed global net ocean budget implies that, when used as input to an atmospheric transport model, the prediction removes an appropriate mass of carbon from the simulated atmosphere: this is an important asset for greenhouse gas monitoring.

The latest model version, FFNNv2022, was ultimately used to predict  $f\text{CO}_2$  from January 2022 to August 2023, that is, up to 20 months beyond the coverage of its training data set. This study also exemplified the assessment of air-sea CO<sub>2</sub> fluxes ( $fg\text{CO}_2$ ) generated from the predicted  $f\text{CO}_2$  in the years 2022–2023 over the eastern tropical Pacific, where regional CO<sub>2</sub> gas exchanges greatly vary with El Niño–Southern Oscillation (ENSO) conditions and thus substantially affect interannual variability of the global net sink. The year 2022 has been predicted with persistently high  $f\text{CO}_2$  (strong CO<sub>2</sub> outgassing to the atmosphere) in response to the maintenance of La Niña since summer 2020. A remarkable reduction in the tropical Pacific CO<sub>2</sub> source in August 2023 relative to the year before coincides with the weakening of the cooling phase. Recent discussions about the interaction between the ocean and climate have dominantly focused on returning El Niño events, their high possibility in triggering more extreme heat worldwide, and further impacts on the marine carbon cycle by the end of 2023 onwards. However, already in June 2023, exceptional surface ocean warming and extraordinarily low wind intensity appeared with

values falling out of historical records over the northeastern Atlantic ocean. Correspondingly, we have found an anomalous reduction in CO<sub>2</sub> uptake setting this regional sink back to its magnitude in the 2000s. These results emphasize critical needs and open the possibility to derive monthly predictions for global surface ocean maps of numerous variables driven by fCO<sub>2</sub>, including air-sea fluxes, seawater pH, and dissolved inorganic carbon, as the reconstruction quality of fCO<sub>2</sub> drives that of the other variables (Chau et al., 2022a, 2022b). The new data sets for the year 2022 (January) to 2023 (August) are available via the LSCE data center (see Section Data availability) and are updated each month. This demonstration of an operational service will be extended at an increased horizontal resolution, following the current development of the reference CMEMS-LSCE-FFNN reconstructions (Chau et al., 2024).

## Data Availability Statement

Data provided in this research are available for use with open access granted by the French LSCE Data Center ([https://dods.lsce.ipl.fr/invsat/FFNN\\_low-latency/](https://dods.lsce.ipl.fr/invsat/FFNN_low-latency/)).

## Acknowledgments

We acknowledge funding support by the MOB TAC project of the European Copernicus Marine Environment Monitoring Service (CMEMS, <https://marine.copernicus.eu/about/producers/mob-tac>, last access: 20/09/2023). SOCAT is an international effort endorsed by the International Ocean Carbon Coordination Project (IOCCP), the Surface Ocean Lower Atmosphere Study (SOLAS) and the Integrated Marine Biogeochemistry and Ecosystem Research program (IMBER), to deliver a uniformly quality-controlled surface ocean CO<sub>2</sub> database. The LSCE data center has offered data repository and access. We thank François-Marie Bréon for the tool development of xCO<sub>2</sub> extrapolation and comments on the first manuscript version and we thank Cédric Bacour for his help in running the extrapolation tool. We are grateful to the two reviewers for their comments and suggestions to refine the manuscript.

## References

- Bakker, D., Alin, S., Becker, M., Bittig, H., Castaño-Primo, R., Feely, R. A., et al. (2022). SOCAT version 2022 for quantification of ocean CO<sub>2</sub> uptake [Dataset]. SOCAT. <https://doi.org/10.25921/1h9f-nb73>
- Bakker, D., Alin, S., Castaño-Primo, R., Margot, C., Gritzalis, T., Kozyr, A., et al. (2021). SOCAT version 2021 for quantification of ocean CO<sub>2</sub> uptake [Dataset]. SOCAT. <https://sodat.info/index.php/version-2021/>
- Bakker, D., Alin, S. R., Bates, N., Becker, M., Feely, R. A., Gkritzalis, T., et al. (2023). Surface ocean CO<sub>2</sub> atlas database version 2023 (SOCATV2023) [Dataset]. SOCAT. <https://doi.org/10.25921/r7xa-bt92>
- Bakker, D., Pfeil, B., Landa, C. S., Metzl, N., O'Brien, K. M., Olsen, A., et al. (2016). A multi-decade record of high-quality fCO<sub>2</sub> data in version 3 of the surface ocean CO<sub>2</sub> atlas (SOCAT). *Earth System Science Data*, 8(2), 383–413. <https://doi.org/10.5194/essd-8-383-2016>
- Bates, N. R., Astor, Y. M., Church, M. J., Currie, K., Dore, J. E., González-Dávila, M., et al. (2014). A time-series view of changing surface ocean chemistry due to ocean uptake of anthropogenic CO<sub>2</sub> and ocean acidification. *Oceanography*, 27(1), 126–141. <https://doi.org/10.5670/oceanog.2014.16>
- Canadell, J. G., Monteiro, P. M., Costa, M. H., Da Cunha, L. C., Cox, P. M., Alexey, V., et al. (2021). *Global carbon and other biogeochemical cycles and feedbacks in climate change 2021: The physical science basis. Contribution of working group I to the sixth assessment report of the intergovernmental panel on climate change*. Cambridge University Press. <https://doi.org/10.1017/9781009157896.007>
- Chau, T. T. T., Gehlen, M., & Chevallier, F. (2022a). Global ocean surface carbon product (Research Report No. CMEMS-MOB-QUID-015-008) [Dataset]. Le Laboratoire des Sciences du Climat et de l'Environnement. <https://doi.org/10.48670/moi-00047>
- Chau, T. T. T., Gehlen, M., & Chevallier, F. (2022b). A seamless ensemble-based reconstruction of surface ocean pCO<sub>2</sub> and air-sea CO<sub>2</sub> fluxes over the global coastal and open oceans. *Biogeosciences*, 19(4), 1087–1109. <https://doi.org/10.5194/bg-19-1087-2022>
- Chau, T. T. T., Gehlen, M., Metzl, N., & Chevallier, F. (2024). CMEMS-LSCE: A global, 0.25°, monthly reconstruction of the surface ocean carbonate system. *Earth System Science Data*, 16, 121–160. <https://doi.org/10.5194/essd-2023-146>
- Fay, A. R., & McKinley, G. A. (2014). Global open-ocean biomes: Mean and temporal variability. *Earth System Science Data*, 6(2), 273–284. <https://doi.org/10.5194/essd-6-273-2014>
- Friedlingstein, P., O'Sullivan, M., Jones, M. W., Andrew, R. M., Gregor, L., Hauck, J., et al. (2022). Global carbon budget 2022. *Earth System Science Data*, 14(11), 4811–4900. <https://doi.org/10.5194/essd-14-4811-2022>
- Gallego, M., Timmermann, A., Friedrich, T., & Zeebe, R. E. (2018). Drivers of future seasonal cycle changes in oceanic pCO<sub>2</sub>. *Biogeosciences*, 15(17), 5315–5327. <https://doi.org/10.5194/bg-15-5315-2018>
- Gregor, L. (2022). REgional Carbon Cycle Assessment and Processes2 biomes [Dataset]. GitHub. Retrieved from <https://github.com/RECCAP2-ocean/RECCAP2-shared-resources/tree/master/data/regions>
- Gregor, L., & Gruber, N. (2021). Oceansoda-Ethz: A global gridded data set of the surface ocean carbonate system for seasonal to decadal studies of ocean acidification. *Earth System Science Data*, 13(2), 777–808. <https://doi.org/10.5194/essd-13-777-2021>
- Gregor, L., Lebehot, A. D., Kok, S., & Scheel Monteiro, P. M. (2019). A comparative assessment of the uncertainties of global surface ocean CO<sub>2</sub> estimates using a machine-learning ensemble (CSIR-ML6 version 2019a) – Have we hit the wall? *Geoscientific Model Development*, 12(12), 5113–5136. <https://doi.org/10.5194/gmd-12-5113-2019>
- Gruber, N., Bakker, D. C., DeVries, T., Gregor, L., Hauck, J., Landschützer, P., et al. (2023). Trends and variability in the ocean carbon sink. *Nature Reviews Earth & Environment*, 4(2), 119–134. <https://doi.org/10.1038/s43017-022-00381-x>
- Gruber, N., Landschützer, P., & Lovenduski, N. S. (2019). The variable southern ocean carbon sink. *Annual Review of Marine Science*, 11(1), 159–186. <https://doi.org/10.1146/annurev-marine-121916-063407>
- Janssens-Maenhout, G., Pinty, B., Dowell, M., Zunker, H., Andersson, E., Balsamo, G., et al. (2020). Toward an operational anthropogenic CO<sub>2</sub> emissions monitoring and verification support capacity. *Bulletin of the American Meteorological Society*, 101(8), E1439–E1451. <https://doi.org/10.1175/bams-d-19-0017.1>
- Landschützer, P., Gruber, N., & Bakker, D. C. (2016). Decadal variations and trends of the global ocean carbon sink. *Global Biogeochemical Cycles*, 30(10), 1396–1417. <https://doi.org/10.1002/2015gb005359>
- Landschützer, P., Ilyina, T., & Lovenduski, N. S. (2019). Detecting regional modes of variability in observation-based surface ocean pCO<sub>2</sub>. *Geophysical Research Letters*, 46(5), 2670–2679. <https://doi.org/10.1029/2018gl081756>
- Regnier, P., Resplandy, L., Najjar, R. G., & Ciais, P. (2022). The land-to-ocean loops of the global carbon cycle. *Nature*, 603(7901), 401–410. <https://doi.org/10.1038/s41586-021-04339-9>
- Rödenbeck, C., Bakker, D. C. E., Gruber, N., Iida, Y., Jacobson, A. R., Jones, S., et al. (2015). Data-based estimates of the ocean carbon sink variability – First results of the surface ocean pCO<sub>2</sub> mapping intercomparison (SOCOM). *Biogeosciences*, 12(23), 7251–7278. <https://doi.org/10.5194/bg-12-7251-2015>

- Rödenbeck, C., Keeling, R. F., Bakker, D. C., Metzl, N., Olsen, A., Sabine, C., & Heimann, M. (2013). Global surface-ocean  $p\text{CO}_2$  and sea-air  $\text{CO}_2$  flux variability from an observation-driven ocean mixed-layer scheme. *Ocean Science*, 9(2), 193–216. <https://doi.org/10.5194/os-9-193-2013>
- Rustogi, P., Landschützer, P., Brune, S., & Baehr, J. (2023). The impact of seasonality on the annual air-sea carbon flux and its interannual variability. *npj Climate and Atmospheric Science*, 6(1), 66. <https://doi.org/10.1038/s41612-023-00378-3>
- Takahashi, T., Sutherland, S. C., Sweeney, C., Poisson, A., Metzl, N., Tilbrook, B., et al. (2002). Global sea-air  $\text{CO}_2$  flux based on climatological surface ocean  $p\text{CO}_2$ , and seasonal biological and temperature effects. *Deep Sea Research Part II: Topical Studies in Oceanography*, 49(9–10), 1601–1622. [https://doi.org/10.1016/s0967-0645\(02\)00003-6](https://doi.org/10.1016/s0967-0645(02)00003-6)